ADVANCED MATERIALS

Angle-Dependent Extinction of Anisotropic Silica/Au Core/Shell Colloids Made via Ion Irradiation**

By *Joan J. Penninkhof*, *Christina Graf*, *Teun van Dillen*, *Arjen M. Vredenberg*, *Alfons van Blaaderen*, and *Albert Polman**

Metallo-dielectric colloids, consisting of a metal and a dielectric material in a core/shell geometry, form a new class of interesting building blocks for photonic materials. Coherent oscillations of the conduction electrons in the metal give rise to strong plasmon resonances. The plasmon frequency depends on the size, shape, and composition of the metal, and the optical constant of the surrounding medium. For metal shells, the optical response also depends on the relative ratio of the core radius and the shell thickness. By variation of this core-to-shell ratio, the plasmon frequency can be shifted from the visible into the infrared region of the spectrum (2.3 eV to 0.1 eV).[1–3]

While many papers have been published on spherical core/shell systems, *anisotropic* composite colloids give an additional parameter for tailoring the optical response. Control over the shape of the anisotropic composite particles is of great importance, for example in studies of electro-magnetic field enhancements near highly curved metal surfaces. One approach to synthesize monodisperse anisotropic core/shell particles with a metal shell is seeded growth, as was shown recently by Limmer et al.[4] for silica and titania nanorods. Another approach, as will be shown in this paper, is to use ion irradiation to change the shape of colloids from spherical to (oblate) ellipsoidal.

Over the last few years, ion-beam-induced plastic deformation of colloidal particles has been addressed in several papers.[5–7] It was shown that colloids expand biaxially perpendicular to the ion-beam direction and contract uniaxially along the ion-beam direction, while their volume remains constant. The aspect ratio of the ellipsoids can be accurately tuned by varying the ion fluence. This plastic deformation is known to occur in amorphous materials, with the deformation rate dependent on the electronic energy loss of the penetrating ions. Ion irradiation is a directional technology; the ellipsoidally shaped colloids are thus all aligned along the ion-beam direction. This enables optical characterization by averaging over large ensembles. The deformed particles can also be removed from the substrate and brought back into solution by sonication.[5] Depending on the irradiation conditions and the desired aspect ratio, the particle yield is typically 10^8–10^9 particles (0.5–5 mg) per hour.

Recently, ion irradiation was applied to metallo-dielectric colloids comprising a Au core and a silica shell.[8] It was found that the irradiation turned the spherical silica shells into oblate ellipsoids and the spherical metal cores into prolate ellipsoids. Au cores without a silica shell remained spherical under ion irradiation.

In this paper we demonstrate that colloids of the reverse core/shell geometry, i.e., colloids consisting of a silica core (diameter: 300–500 nm) and an Au shell (thickness: 20–60 nm), also show plastic deformation upon ion irradiation. The shape of the spherical colloids changed into oblate ellipsoidal, with the final degree of anisotropy determined by the ion fluence. The observed deformation is attributed to the ion-induced anisotropic deformation process in the amorphous silica. At constant fluence, we find that the net observed anisotropy decreases with increasing Au-shell thickness, indicating that the Au shell imposes a mechanical constraint on the deformation of the silica core. Optical transmission measurements on deformed silica/Au/silica core/shell/shell colloids on glass show that the extinction spectra are strongly angle-dependent, with a peak shift of 700 nm.

Figure 1a shows a side-view scanning electron microscopy (SEM) image (10°-tilt angle) of Au-shell colloids before ion irradiation. The angle of irradiation and the view angles are indicated in the scheme in the top left of Figure 1. The total diameter of the colloids is 530 nm with an absolute polydispersity of 18 nm; the Au shell is (46 ± 11) nm thick. Next, the sample was irradiated with 30 MeV Cu ions to a fluence of 5×10^{14} ions cm^{-2} at 45°. Figure 1b shows irradiated colloids, imaged along the ion-beam direction. The dashed circle indicates the circumference of the unirradiated particles. It is clear that the colloids have expanded in the direction perpendicular to the ion beam. In Figure 1c, the colloids are imaged almost perpendicular to the ion-beam direction, at a side-view tilt angle of 10° with respect to the substrate surface. Clearly, the colloids have contracted along the ion beam. The silica core remains uniformly covered with Au after deformation. These irradiated colloids have an average size aspect ratio (major over minor diameter) of 1.47 ± 0.16.

The ion-irradiation-induced plastic deformation of amorphous materials can be described by a viscoelastic thermal spike model.[9,10] An energetic ion that penetrates a solid

[*] Prof. A. Polman, Dr. T. van Dillen,[+] J. J. Penninkhof
Center for Nanophotonics, FOM Institute AMOLF
Kruislaan 407, NL-1098 SJ Amsterdam (The Netherlands)
E-mail: polman@amolf.nl
Dr. C. Graf,[++] Prof. A. van Blaaderen
Soft Condensed Matter, Debye Institute, Utrecht University
P.O. Box 80000, NL-3508 TA Utrecht (The Netherlands)
Dr. A. M. Vredenberg
Functional Materials, Debye Insitute, Utrecht University
P.O. Box 80000, NL-3508 TA Utrecht (The Netherlands)
[+] Present address: Applied Physics, University of Groningen, Nijenborgh 4, NL-9747 AG Groningen, The Netherlands.
[++] Present address: Institut für Physikalische Chemie, Universität Würzburg, Am Hubland, D-97074 Würzburg, Germany.

[**] The authors gratefully acknowledge Prof. Dr. L. W. Jenneskens and Dr. C. A. van Walree (UU) for the use of the CARY 5 spectrophotometer. This work is part of the research program of the "Stichting voor Fundamenteel Onderzoek der Materie (FOM)", which is financially supported by the "Nederlandse organisatie voor Wetenschappelijk Onderzoek (NWO)". J. J. Penninkhof and C. Graf contributed equally to the work.

  DOI: 10.1002/adma.200401742

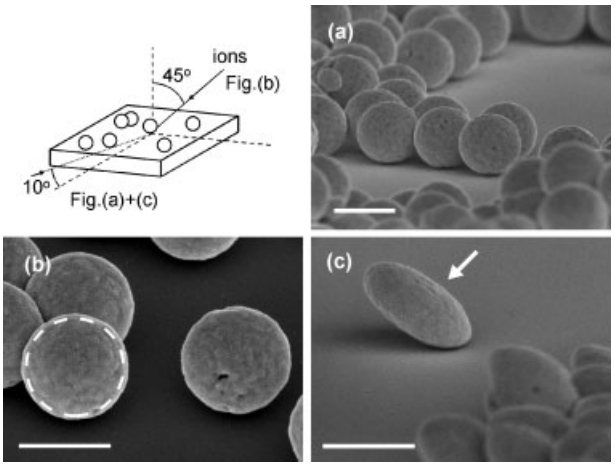

Figure 1. SEM images of silica-core/Au-shell colloids on a silicon substrate: a) unirradiated, b,c) irradiated with 30 MeV Cu ions at 45° at 77 K to a fluence of 5×10^{14} ions cm^{-2}, viewing angle parallel (b) or almost perpendicular (c) to the ion-beam direction. The upper-left scheme shows the ion-beam direction and the SEM viewing angles. Scale bars are 500 nm.

heats a small cylindrical region along the ion track in less than 10^{-12} s. The rapid thermal expansion of this thermal spike causes deviatoric (shear) stresses that relax by Newtonian viscous flow at ion-track temperatures above the flow temperature. It is accompanied by the generation of viscous strains that freeze in for large track cooling rates, resulting in a net local anisotropic deformation of the material. The macroscopic deformation then is the result of many ion impacts in each colloid. For the fluence and colloids of Figure 1, a typical number of 10^6 ions impacted on each colloid. In contrast to amorphous materials such as silica, crystalline materials do not show anisotropic deformation under ion irradiation.[11,12] This effect is attributed to epitaxial recrystallization at the solid–liquid interface of the molten cylindrical thermal spike region. In addition, track temperatures in crystalline metals are not likely to exceed the melting temperature as a result of rapid redistribution of the deposited energy in the electronic subsystem.[13,14] Given the deformation observed in Figure 1, the deforming silica core must thus impose a deformation on the Au shell that would otherwise not deform under irradiation. We attribute the conformal shape transformation of the metal to radiation-induced viscous flow that leads to an effective softening of the metal under irradiation. Metals such as Al and W are known to relax stress by ion-irradiation-induced Newtonian viscous flow.[15,16] This is further supported by the observation that the metal-shell surface appears somewhat smoothened after the irradiation (see Figs. 1c, 2b). We remark that the radiation-induced flow of the metal is thus of entirely different nature than the anisotropic strain generation that leads to plastic deformation of the silica.[17]

To directly compare the deformation of core/shell colloids with that of pure silica colloids (i.e., without an Au shell), droplets of both colloidal suspensions were dried on a silicon substrate. The average radii of the silica colloids and silica/Au colloids were (149 ± 4) nm and (173 ± 6) nm, respectively. The average thickness of the Au shell thus amounts to (24 ± 7) nm. Figure 2a shows a top-view SEM image of a silica colloid (left) and a silica/Au colloid (right). After irradiation with 30 MeV Cu ions to a fluence of 1×10^{15} ions cm^{-2} at normal incidence the same two colloids were imaged again, as shown

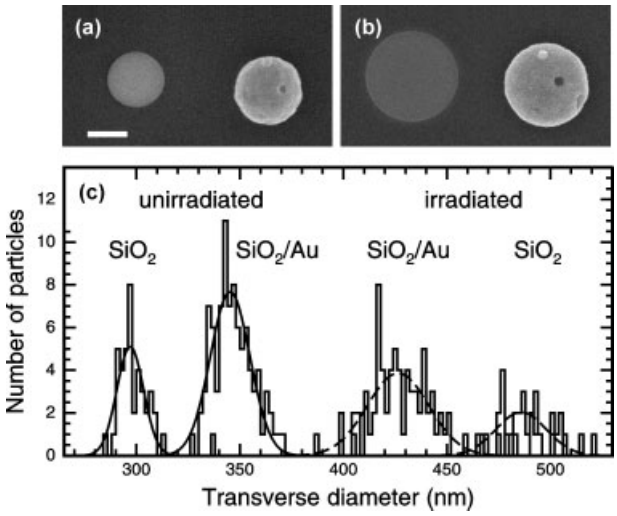

Figure 2. a,b) Top-view SEM images of the same colloids (a silica-core colloid and a silica/Au colloid) before (a) and after (b) irradiation with 30 MeV Cu ions at normal incidence to a fluence of 1×10^{15} ions cm^{-2}. The scale bar is 200 nm. c) Histograms of the transverse diameter of Au-shell colloids and silica reference colloids before (lines) and after (dashed lines) irradiation.

in Figure 2b. Note that the nanoscale features (e.g., the hole) of the Au shell are preserved. As expected, the transverse dimensions of both types of colloids have increased. However, the transverse diameter of the silica colloid is now larger than that of the silica/Au colloid. Figure 2c shows the distributions of the transverse diameter of the colloids before and after the ion irradiation. Gaussian fits through these data show that the average transverse diameter of the silica colloids increased from (297 ± 6) nm to (486 ± 12) nm, while the average transverse diameter of silica/Au colloids increased from (345 ± 10) nm to (426 ± 15) nm. From this, we conclude that the presence of the Au shell reduces the ion-beam-induced anisotropic deformation of the silica core.

To examine the effect of the Au-shell thickness on the deformation process in more detail, silica/Au colloids were synthesized using identical silica cores of radius (217 ± 10) nm and varying Au-shell thickness. After the synthesis, the thicknesses of the Au shell were found to be (25 ± 13) nm, (47±10) nm, and (58±10) nm. A 30 MeV Cu beam at an angle of 45° was used to deform the colloids. The fluence was 1×10^{15} ions cm^{-2}. In Figure 3 the average transverse diameter $<L>$ is plotted versus the thickness of the Au shell. The data were normalized to the average diameter $<L_0>$ before irradiation. We observe

ADVANCED MATERIALS

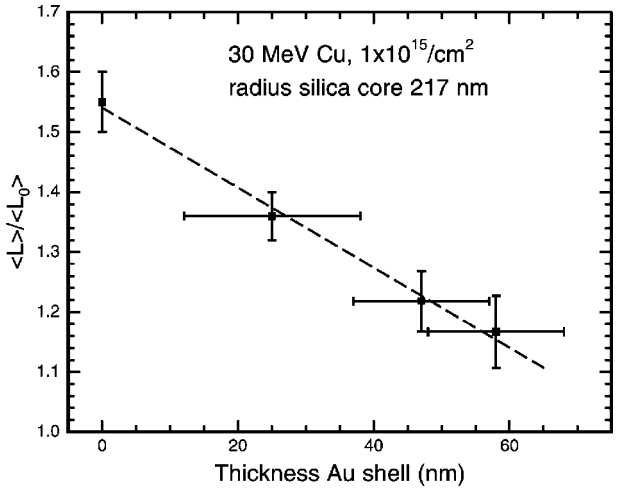

Figure 3. Averaged normalized transverse diameter versus Au-shell thickness for silica/Au colloids irradiated with 30 MeV Cu to a fluence of 1×10^{15} ions cm^{-2}. The observed deformation is reduced upon an increase in Au-shell thickness. The dashed line is a guide to the eye.

that the anisotropic deformation decreases upon an increase of the thickness of the Au shell.

It is by now quite well established that the electronic stopping S_e of the energetic ions is responsible for the ion-beam-induced plastic deformation of amorphous materials like silica.[18,19] The decrease in S_e in the silica owing to the energy loss in the Au shell is only 1 % for the dimensions under consideration.[20] The reduced deformation of the silica core must thus be due to the mechanical constraint of the metal shell. Indeed, for very large shell thicknesses, no deformation of the core is expected. Our data in Figure 3 predict this to occur for Au shells on silica colloids (with a radius of 217 nm) thicker than about 100 nm.

It is interesting to compare our data with those by Garrido et al., who studied multilayered systems composed of a crystalline layer of Au or W sandwiched between two layers of amorphous Ni_3B.[21] Upon ion irradiation with 500 MeV I ions, they observed that the crystalline layer was subjected to a tensile stress owing to the expanding adjacent amorphous layer. In this case, the metal layer then counteracts the expansion of the amorphous layers by means of macroscopic elastic forces. It was found that the net deformation decreased with thickness of the crystalline layer, similar to our experiments.

Next, we investigated the plastic deformation of silica colloids covered with an Au shell and an additional silica shell. This outer silica shell is useful in preventing aggregation of the metal-shell colloids during growth and drying of colloidal crystals (by reduction of the van der Waals forces). It could also serve as a host for optical emitters such as dyes, rare-earth ions, or quantum dots, whose emission is modified by the local field enhancements. The thickness of this outer silica shell was either (44 ± 7) nm or (133 ± 7) nm. The Au-shell colloids consisted of a silica core with a radius of (149 ± 4) nm covered with a (24 ± 7) nm thick Au shell. Silica colloids of different sizes, made using seeded Stöber growth, were used as a reference for the deformation experiments. The colloids were irradiated with 6 MeV Au ions to a fluence of 6.5×10^{14} ions cm^{-2} at an angle of 45° at 77 K. The resulting deformation of the colloids versus the colloid diameter before irradiation is shown in Figure 4. The core/shell/shell structure of the colloids is schematically depicted as well.

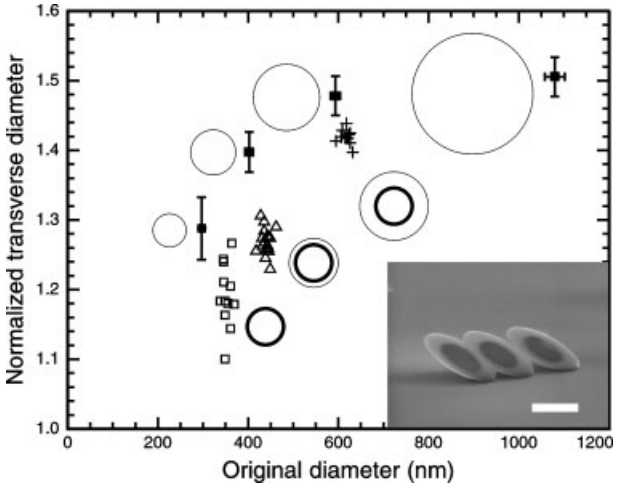

Figure 4. Normalized transverse diameter versus the original diameter of the silica and the silica-core/Au-shell/silica-shell colloids after irradiation with 6.5×10^{14} Au cm^{-2} at an angle of 45°: silica (closed squares), silica/Au (open squares), and silica/Au colloids with an outer silica shell (open triangles/crosses). The core/shell/shell structure of the colloids is also indicated in schematics. A side-view SEM image of irradiated Au-shell colloids with a thick silica shell is shown as inset. The scale bar is 500 nm.

Three conclusions can be drawn from this graph. Firstly, for pure silica colloids (closed squares) the ion-beam-induced anisotropic deformation decreases with decreasing diameter. As will be shown in a separate paper, this effect is due to capillary stresses resulting from the surface tension.[22] Secondly, as was already shown in this paper, Au-shell colloids (open squares) show a reduced deformation compared to the corresponding silica-core colloids (closed squares, diameter 300 nm). The spread in the data reflects the polydispersity of the shell thickness. Thirdly, Au-shell colloids with an additional silica shell (open triangles, crosses) deform less than pure silica colloids of equal size, but for increasing silica-shell thickness, the overall deformation approaches that of pure silica colloids. The inset in Figure 4 shows a side-view SEM image of irradiated Au-shell colloids with thick silica shells. In the image, taken using a 30 keV electron beam, the embedded (deformed) Au shell appears as a clear contrast. This is a result of the backscattered electrons of the substrate and the Au shell that generate additional secondary electrons, which then are both detected. Owing to the sensitivity of the backscattered electrons to the tilt angle of the sample, the inverse contrast can be observed as well (for example at normal incidence).

Preliminary optical transmission measurements were performed with unpolarized light to determine the effect of the shape anisotropy on the extinction spectra. A dilute colloidal suspension was dried onto positively charged glass substrates (using poly(allylamine hydrochloride)), yielding a sub-monolayer coverage. The colloids consisted of a silica core with a radius of 228 nm covered with a 38 nm thick Au shell and a 60 nm thick outer silica shell. One sample was irradiated with 4 MeV Xe ions at an angle of 45° to a fluence of 1×10^{15} ions cm^{-2}. After irradiation, the average aspect ratio of the colloids was measured with SEM and found to be 1.8 ± 0.2. Next, the samples were immersed in index-matching oil ($n = 1.51$). Normalized transmission spectra of this sample are shown in Figure 5a for different angles of the incident light beam with respect to the surface normal. The angle was varied from +45° (spectrum b, light along the ion-beam direction) to –45° (spectrum h, perpendicular to the ion beam) in steps of 15°. As a reference, spectrum a in Figure 5a shows the transmission of a sample with undeformed colloids. We observe that the spectra of the deformed colloids are broader and angle-dependent: the maximum in extinction shifts to the infrared for angles more perpendicular to the ion-beam direction. This shift is clearly seen in Figure 5b, were the extinction maxima are plotted as a function of angle of incidence. We observe that the extinction maximum shifts from ~700 nm to almost 1400 nm. Future work will focus on the influence of aspect ratio and the use of polarized light, as well as on calculations of the optical properties of anisotropic core/shell particles.

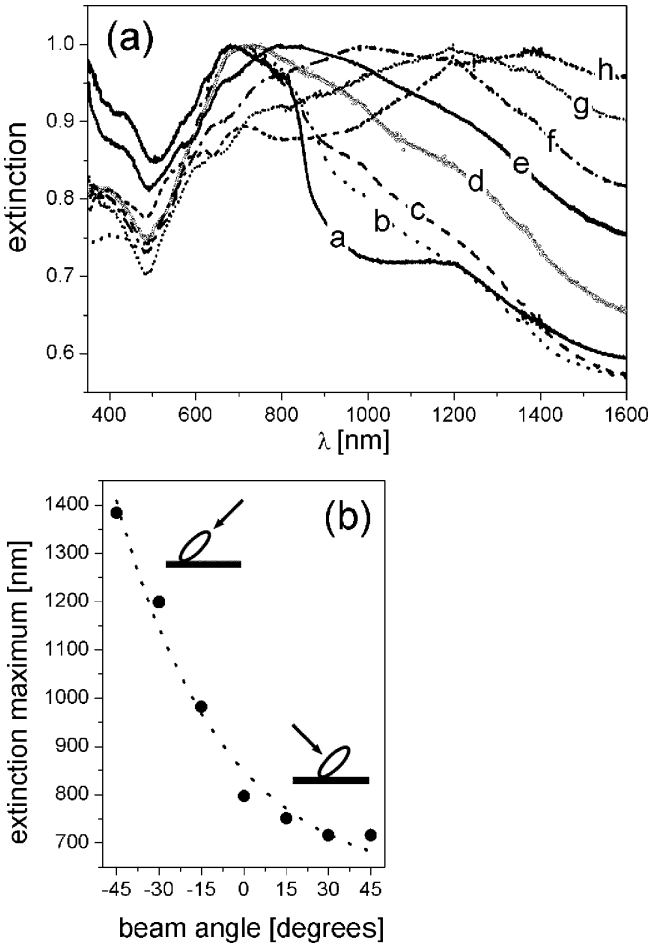

Figure 5. a) Optical transmission spectra of deformed silica spheres (228 nm radius) with an Au shell (38 nm) and an outer silica shell (60 nm) as a function of angle of the incident light beam. The angle was varied from 45° (i.e., parallel to ion-beam direction, spectrum b) to –45° (i.e., perpendicular to the ion beam direction, spectrum h) in steps of 15°. The transmission spectrum for undeformed colloids is shown as spectrum a. The maxima of the spectra in (a) are plotted in (b) as a function of the angle of the incident optical beam.

In summary, we have shown that MeV ion irradiation can be used to turn spherical colloids with a silica core and a metal shell into oblate ellipsoids. A typical major-to-minor aspect ratio of 1.5 is achieved after irradiation with 30 MeV Cu to a fluence of 5×10^{14} ions cm^{-2}. The anisotropic plastic deformation is attributed to the ion-induced deformation of the silica core, counteracted by the mechanical constraint of the metal shell. At constant fluence, an increase of the metal-shell thickness reduces the deformation, while the addition of an extra silica shell results in deformation rates that approach the deformation rates of silica. Optical transmission spectra measured on a sample with anisotropic metal-shell particles are highly angle-dependent. Due to the high level of control over the aspect ratio, these anisotropic metallo-dielectric colloids may be ideal building blocks in photonic applications.

Experimental

Materials: Silica/Au colloids were synthesized using the method described elsewhere [23]. In brief, monodisperse silica colloids with diameters in the range between 300 nm and 500 nm were synthesized using the Stöber method [24] and functionalized with 3-aminopropyltrimethoxysilane to enable the attachment of small gold nanoclusters (1–2 nm in diameter). The Au shell was grown via reduction of an aged solution of chloroauric acid by addition of a hydroxylamine hydrochloride solution. The thickness of the Au shell was controlled by the ratio of the amount of precursor particles and the volume of the gold salt solution. Thicker Au shells were grown by seeded growth. An additional outer silica shell was grown via functionalization of the silica/Au particles by polyvinylpyrrolidone [25], after which the colloids were transferred into ethanol to enable Stöber growth. After synthesis, a droplet of the colloidal suspension was dried on a Si(100) substrate under nitrogen flow, so that the typical surface coverage was well below a monolayer.

Ion Irradiation: Ion irradiation was performed using a 1 MV and a 6 MV Van de Graaff accelerator. The ion beam was electrostatically scanned across a 1.0 cm × 1.0 cm area. Ion beams of 30 MeV Cu^{5+}, 6 MeV Au^{3+}, and 4 MeV Xe^{4+} were used either at normal incidence or at an angle of 45° with respect to the substrate normal. In principle, any energy and species can be chosen to induce plastic deformation, although the deformation rate is higher for increasing electronic stopping. Practically, the ion beam is limited by the type of accelerator (ion yield) and the source material. The ion-beam energy flux was in the range of 0.04–0.9 W cm^{-2} for all irradiations. During the irradiation, the samples were clamped to a liquid-nitrogen-cooled Cu substrate holder.

ADVANCED MATERIALS

Characterization: SEM at 5–30 keV was used to determine the particles' size and shape before and after ion irradiation. Optical transmission spectra were measured using a Varian Cary 5 spectrophotometer.

Received: October 22, 2004
Final version: February 17, 2005

[1] U. Kreibig, M. Vollmer, *Optical Properties of Metal Clusters*, Springer, Berlin, Germany **1995**.
[2] C. F. Bohren, D. R. Huffman, *Absorption and Scattering of Light by Small Particles*, Wiley, New York **1983**.
[3] S. J. Oldenburg, R. D. Averitt, S. L. Westcott, N. J. Halas, J. L. West, *Chem. Phys. Lett.* **1998**, *288*, 243.
[4] S. J. Limmer, T. P. Chou, G. Cao, *J. Phys. Chem. B* **2003**, *107*, 13 313.
[5] E. Snoeks, A. van Blaaderen, T. van Dillen, C. M. van Kats, K. P. Velikov, M. Brongersma, A. Polman, *Nucl. Instrum. Methods Phys. Res. Sect. B* **2001**, *178*, 62.
[6] T. van Dillen, A. Polman, W. Fukarek, A. van Blaaderen, *Appl. Phys. Lett.* **2001**, *78*, 910.
[7] S. Klaumünzer, *Nucl. Instrum. Methods Phys. Res. Sect. B* **2004**, *215*, 345.
[8] S. Roorda, T. van Dillen, A. Polman, C. Graf, A. van Blaaderen, B. J. Kooi, *Adv. Mater.* **2004**, *16*, 235.
[9] H. Trinkaus, A. I. Ryazanov, *Phys. Rev. Lett.* **1995**, *74*, 5072.
[10] T. van Dillen, A. Polman, P. R. Onck, E. van der Giessen, *Phys. Rev. B* **2005**, *71*, 024 103.
[11] M. Hou, S. Klaumünzer, G. Schumacher, *Phys. Rev. B* **1990**, *41*, 1144.
[12] T. van Dillen, M. J. A. de Dood, J. J. Penninkhof, A. Polman, S. Roorda, A. M. Vredenberg, *Appl. Phys. Lett.* **2004**, *84*, 3591.
[13] Z. G. Wang, C. Dufour, E. Paumier, M. Toulemonde, *J. Phys. Condens. Matter* **1994**, *6*, 6733.
[14] Y. Yavlinskii, *Nucl. Instrum. Methods Phys. Res. Sect. B* **1998**, *146*, 142.
[15] C. A. Volkert, A. Polman, *Mater. Res. Soc. Symp. Proc.* **1992**, *235*, 3.
[16] E. Snoeks, K. S. Boutros, J. Barone, *Appl. Phys. Lett.* **1997**, *71*, 267.
[17] E. Snoeks, T. Weber, A. Cacciato, A. Polman, *J. Appl. Phys.* **1995**, *78*, 4723.
[18] A. Benyagoub, S. Klaumünzer, L. Thomé, J. C. Dran, F. Garrido, A. Dunlop, *Nucl. Instrum. Methods Phys. Res. Sect. B* **1992**, *64*, 684.
[19] T. van Dillen, A. Polman, C. M. van Kats, A. van Blaaderen, *Appl. Phys. Lett.* **2003**, *83*, 4315.
[20] J. F. Ziegler, J. P. Biersack, U. Littmark, *The Stopping and Range of Ions in Solids*, Pergamon, New York **1985**.
[21] F. Garrido, A. Benyagoub, A. Chamberod, J. C. Dran, A. Dunlop, S. Klaumünzer, L. Thomé, *Nucl. Instrum. Methods Phys. Res. Sect. B* **1996**, *115*, 430.
[22] T. van Dillen, E. van der Giessen, P. R. Onck, A. Polman, unpublished.
[23] C. Graf, A. van Blaaderen, *Langmuir* **2002**, *18*, 524.
[24] W. Stöber, A. Fink, E. Bohn, *J. Colloid Interface Sci.* **1968**, *26*, 62.
[25] C. Graf, D. L. J. Vossen, A. Imhof, A. van Blaaderen, *Langmuir* **2003**, *19*, 6693.

Fabrication Method for Thermoelectric Nanodevices**

By *James R. Lim*, *Jay F. Whitacre*, *Jean-Pierre Fleurial*, *Chen-Kuo Huang*, *Margaret A. Ryan*, and *Nosang V. Myung**

Remarkable results from the evaluation of higher efficiency thermoelectric materials and their properties have reinvigorated interest in the field of thermoelectrics (TEs).[1–4] The efficiency of thermoelectric materials is directly related to the dimensionless figure of merit (ZT).[5] Current and longstanding state-of-the-art thermoelectric materials, at near-room-temperature operation, are Bi_2Te_3-based bulk alloys with ZT values around one.[6] However, to compete for market share against conventional power sources and refrigerators, thermoelectric efficiencies need to be improved to ZT values around three.[5] Nanoarchitectured thermoelectric devices have provided the impetus for higher efficiency materials and new technological advancements in science and engineering.

TEs convert heat into electricity (Seebeck effect) and vice versa (Peltier effect).[5] Thermoelectric devices consist of many n-type and p-type thermoelectric elements connected electrically in series and arranged thermally in parallel. The many advantages of TE devices include solid-state operation, zero emission, vast scalability, no maintenance, and a long operating lifetime. Nonetheless, because of their limited energy-conversion efficiencies, thermoelectrics have a rather specific range of applications. Examples of applications include radioisotope thermoelectric generators (RTGs)[7] for power generation and optoelectronic thermal management for cooling purposes.[8]

Throughout the microelectronics industry, miniaturization has become affordable, versatile, and readily accessible. The

[*] Prof. N. V. Myung
Department of Chemical and Environmental Engineering
Center for Nanoscale Science and Engineering
University of California
Riverside, CA 92521 (USA)
E-mail: myung@engr.ucr.edu
J. R. Lim
Department of Materials Science and Engineering
Biomedical Engineering IDP
University of California
Los Angeles, CA 90095 (USA)
Dr. J. F. Whitacre
Electrochemical Technologies Group
Jet Propulsion Laboratory, California Institute of Technology
4800 Oak Grove Drive, Pasadena, CA 91109 (USA)
Dr. J.-P. Fleurial, Dr. C.-K. Huang, Dr. M. A. Ryan
Materials and Device Technology Group
Jet Propulsion Laboratory, California Institute of Technology
4800 Oak Grove Drive, Pasadena, CA 91109 (USA)

[**] This work was supported by the NASA Code T Bio/Nano Program. The Jet Propulsion Laboratory is an operating division of the California Institute of Technology under contract with the National Aeronautics and Space Administration.

  DOI: 10.1002/adma.200401189